Multi-Particle Simulation Techniques II

Ji Qiang

Accelerator Modeling Program
Accelerator Technology & Applied Physics Division
Lawrence Berkeley National Laboratory

CERN Accelerator School, Thessaloniki, Greece
Nov. 16, 2018

BERKELEY LAB | U.S. DEPARTMENT OF ENERGY | Office of Science | ACCELERATOR TECHNOLOGY & APPLIED PHYSICS DIVISION ATAP

Contrast of Non-Symplectic and Symplectic Integrator

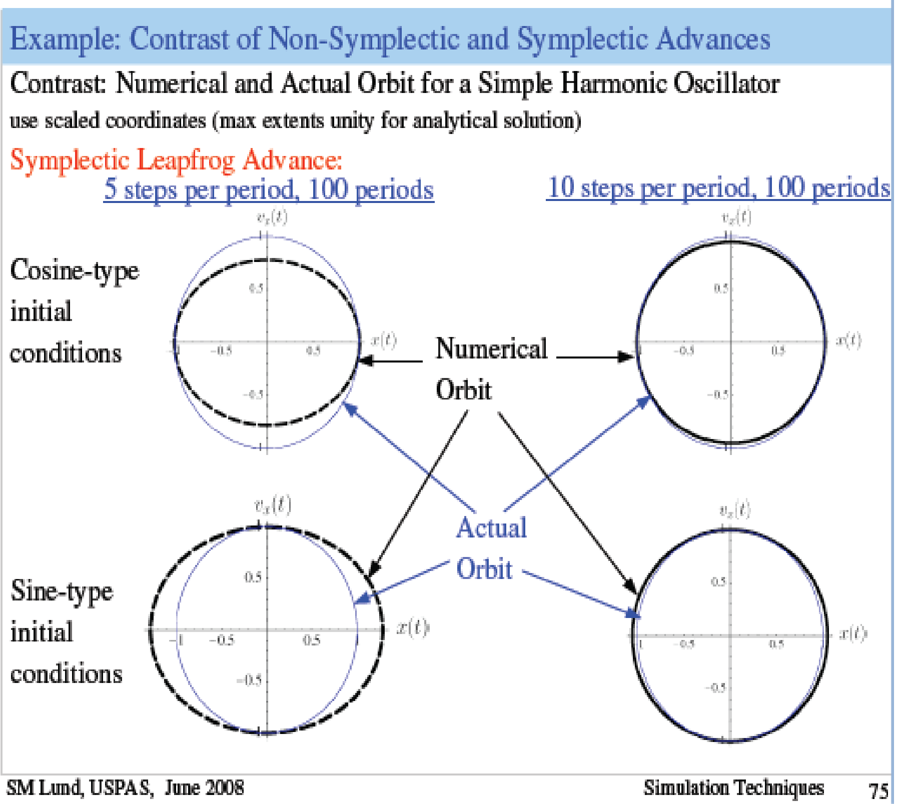

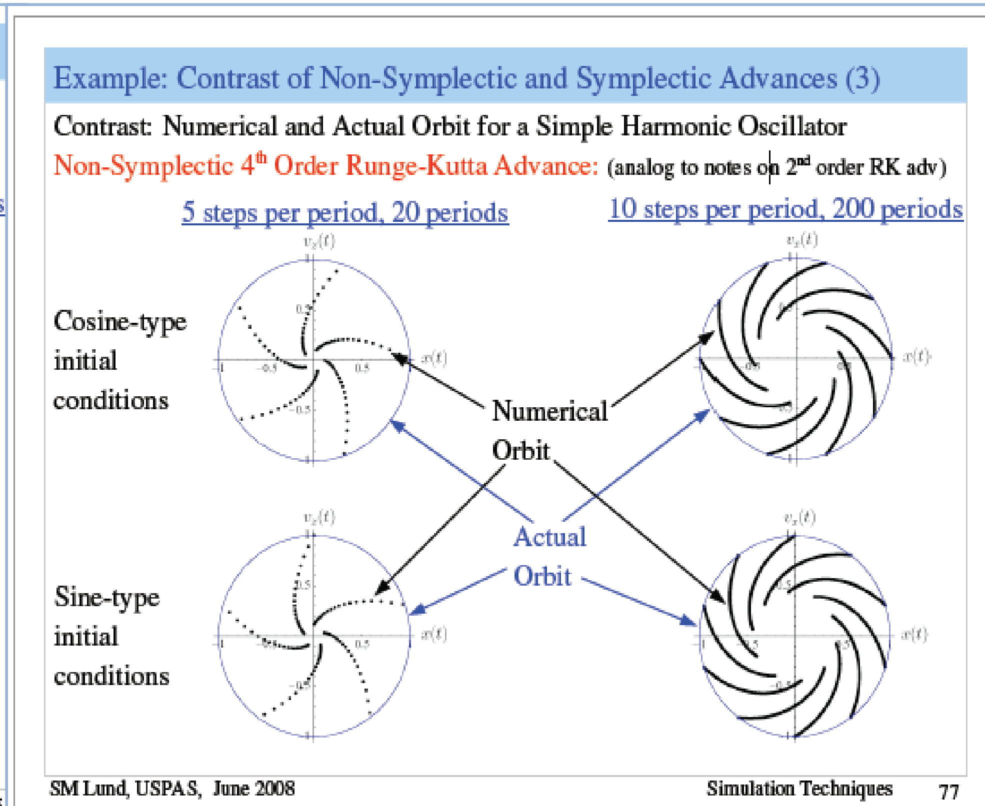

Courtesy of S. Lund

A Symplectic Multi-Particle Tracking Model (1)

multi-particle Hamiltonian $H(\mathbf{r}_1, \mathbf{r}_2, \cdots, \mathbf{p}_1, \mathbf{p}_2, \cdots, s)$

$$H = \sum_i \mathbf{p}_i^2/2 + \frac{1}{2}\sum_i \sum_j q\phi(\mathbf{r}_i, \mathbf{r}_j) + \sum_i q\psi(\mathbf{r}_i)$$

space-charge
Coulomb potential

external focusing/acceleration

$$\frac{d\mathbf{r}_i}{ds} = \frac{\partial H}{\partial \mathbf{p}_i}$$

$$\frac{d\mathbf{p}_i}{ds} = -\frac{\partial H}{\partial \mathbf{r}_i}$$

$$\frac{d\zeta}{ds} = -[H, \zeta]$$

A formal single step solution

$$\zeta(\tau) = \exp(-\tau(:H:))\zeta(0)$$

$\boxed{H = H_1 + H_2}$

$$\zeta(\tau) = \exp(-\tau(:H_1: + :H_2:))\zeta(0)$$
$$= \exp(-\frac{1}{2}\tau :H_1:)\exp(-\tau :H_2:)\exp(-\frac{1}{2}\tau :H_1:)\zeta(0) + O(\tau^3)$$

$$\boxed{\begin{aligned}\zeta(\tau) &= \mathcal{M}(\tau)\zeta(0) \\ &= \mathcal{M}_1(\tau/2)\mathcal{M}_2(\tau)\mathcal{M}_1(\tau/2)\zeta(0)\end{aligned}}$$

$\mathcal{M}$ would be symplectic if both $\mathcal{M}_1$ and $\mathcal{M}_2$ are symplectic

J. Qiang, Phys. Rev. Accel. Beams 20, 014203 (2017), Phys. Rev. Accel. Beams 21, 054201 (2018).

A Symplectic Multi-Particle Tracking Model (2)

2nd order:

$$\begin{aligned}\zeta(\tau) &= \mathcal{M}(\tau)\zeta(0) \\ &= \mathcal{M}_1(\tau/2)\mathcal{M}_2(\tau)\mathcal{M}_1(\tau/2)\zeta(0)\end{aligned}$$

4th order:

$$\mathcal{M}(\tau) = \mathcal{M}_1(\frac{s}{2})\mathcal{M}_2(s)\mathcal{M}_1(\frac{\alpha s}{2})\mathcal{M}_2((\alpha-1)s)\mathcal{M}_1(\frac{\alpha s}{2})\mathcal{M}_2(s)\mathcal{M}_1(\frac{s}{2})$$

where $\alpha = 1 - 2^{1/3}$, and $s = \tau/(1+\alpha)$

higher order:

$$\mathcal{M}_{2n+2}(\tau) = \mathcal{M}_{2n}(z_0\tau)\mathcal{M}_{2n}(z_1\tau)\mathcal{M}_{2n}(z_0\tau)$$

where $z_0 = 1/(2-2^{1/(2n+1)})$ and $z_1 = -2^{1/(2n+1)}/(2-2^{1/(2n+1)})$

Symplectic condition: $\boxed{M_i^T J M_i = J}$ **M is the Jacobi Matrix of $\mathcal{M}$**

where J denotes the $6N \times 6N$ matrix given by

$$J = \begin{pmatrix} 0 & I \\ -I & 0 \end{pmatrix}$$ and I is the $3N \times 3N$ identity matrix

Refs: E. Forest and R. D. Ruth, Physica D **43, p. 105, 1990.** H. Yoshida, Phys. Lett. A **150, p. 262, 1990.**

A Symplectic Multi-Particle Tracking Model (3)

$$H_1 = \sum_i \mathbf{p}_i^2/2 + \sum_i q\psi(\mathbf{r}_i) \longrightarrow \mathcal{M}_1$$

- symplectic map for H_1 can be found from charged particle optics method

$$H_2 = \frac{1}{2}\sum_i \sum_j q\phi(\mathbf{r}_i, \mathbf{r}_j) \longrightarrow \mathcal{M}_2$$

$$\mathbf{r}_i(\tau) = \mathbf{r}_i(0)$$

$$\mathbf{p}_i(\tau) = \mathbf{p}_i(0) - \frac{\partial H_2(\mathbf{r})}{\partial \mathbf{r}_i}\tau$$

$$M_2 = \begin{pmatrix} I & 0 \\ L & I \end{pmatrix}$$

To satisfy the symplectic condition: $\boxed{L = L^T}$

$$L_{ij} = \partial \mathbf{p}_i(\tau)/\partial \mathbf{r}_j = -\frac{\partial^2 H_2(\mathbf{r})}{\partial \mathbf{r}_i \partial \mathbf{r}_j}\tau$$

$\mathcal{M}_2$ will be ***symplectic*** if p_i is updated from H_2 ***analytically***

Self-Consistent Space-Charge Transfer Map (1)

$$\frac{\partial^2\phi}{\partial x^2} + \frac{\partial^2\phi}{\partial y^2} = -\frac{\rho}{\epsilon_0}$$

$$\begin{aligned}\phi(x=0,y) &= 0\\ \phi(x=a,y) &= 0\\ \phi(x,y=0) &= 0\\ \phi(x,y=b) &= 0\end{aligned}$$

$$\rho(x,y) = \sum_{l=1}^{N_l}\sum_{m=1}^{N_m} \rho^{lm}\sin(\alpha_l x)\sin(\beta_m y)$$

$$\phi(x,y) = \sum_{l=1}^{N_l}\sum_{m=1}^{N_m} \phi^{lm}\sin(\alpha_l x)\sin(\beta_m y)$$

$$\rho^{lm} = \frac{4}{ab}\int_0^a\int_0^b \rho(x,y)\sin(\alpha_l x)\sin(\beta_m y)\,dxdy$$

$$\phi^{lm} = \frac{4}{ab}\int_0^a\int_0^b \phi(x,y)\sin(\alpha_l x)\sin(\beta_m y)\,dxdy$$

where $\alpha_l = l\pi/a$ and $\beta_m = m\pi/b$

$$\boxed{\phi^{lm} = \frac{\rho^{lm}}{\epsilon_0\gamma_{lm}^2}}$$ where $\gamma_{lm}^2 = \alpha_l^2 + \beta_m^2$

Self-Consistent Space-Charge Transfer Map (2)

The charge density from macroparticles:

$$\rho(x,y) = \frac{1}{\Delta x \Delta y N_p} \sum_{j=1}^{N_p} S(x - x_j) S(y - y_j)$$

The solution of space-charge potential modes:

$$\phi^{lm} = \frac{4\pi}{\gamma_{lm}^2} \frac{4}{ab} \frac{1}{N_p} \sum_{j=1}^{N_p} \frac{1}{\Delta x \Delta y} \int_0^a \int_0^b S(x - x_j) S(y - y_j) \times \sin(\alpha_l x) \sin(\beta_m y) dx dy \quad ($$

The solution of space-charge potential:

$$\phi(x,y) = 4\pi \frac{4}{ab} \frac{1}{N_p} \sum_{j=1}^{N_p} \sum_{l=1}^{N_l} \sum_{m=1}^{N_m} \frac{1}{\gamma_{lm}^2} \sin(\alpha_l x) \sin(\beta_m y) \frac{1}{\Delta x \Delta y} \int_0^a \int_0^b S(\bar{x} - x_j) S(\bar{y} - y_j) \sin(\alpha_l \bar{x}) \sin(\beta_m \bar{y}) d\bar{x} d\bar{y}.$$

The space-charge potential on macroparticles:

$$\phi(x_i, y_i) = \frac{1}{\Delta x \Delta y} \int_0^a \int_0^b \phi(x,y) S(x - x_i) S(y - y_i) dx dy$$

Self-Consistent Space-Charge Transfer Map (3)

The interaction potential:

$$\varphi(x_i, y_i, x_j, y_j) = 4\pi \frac{4}{ab}\frac{1}{N_p}\sum_{l=1}^{N_l}\sum_{m=1}^{N_m}\frac{1}{\gamma_{lm}^2}\frac{1}{\Delta x \Delta y}\int_0^a\int_0^b S(x-x_j)S(y-y_j)\sin(\alpha_l x)\sin(\beta_m y)dxdy$$
$$\times \frac{1}{\Delta x \Delta y}\int_0^a\int_0^b S(x-x_i)S(y-y_i)\sin(\alpha_l x)\sin(\beta_m y)dxdy.$$

The space-charge Hamiltonian:

$$H_2 = 4\pi \frac{K}{2}\frac{4}{ab}\frac{1}{N_p}\sum_{i=1}^{N_p}\sum_{j=1}^{N_p}\sum_{l=1}^{N_l}\sum_{m=1}^{N_m}\frac{1}{\gamma_{lm}^2}\frac{1}{\Delta x \Delta y}\int_0^a\int_0^b S(x-x_j)S(y-y_j)\sin(\alpha_l x)\sin(\beta_m y)dxdy$$
$$\times \frac{1}{\Delta x \Delta y}\int_0^a\int_0^b S(x-x_i)S(y-y_i)\sin(\alpha_l x)\sin(\beta_m y)dxdy.$$

Symplectic Gridless Symplectic Space-Charge Model

$$\rho(x,y) = \sum_{j=1}^{N_p} w\delta(x-x_j)\delta(y-y_j)$$

w is the particle charge weight

$$H_2 = \frac{1}{2\epsilon_0}\frac{4}{ab} w \sum_i \sum_j \sum_l \sum_m \frac{1}{\gamma_{lm}^2} \sin(\alpha_l x_j) \sin(\beta_m y_j)\sin(\alpha_l x_i)\sin(\beta_m y_i)$$

$\mathcal{M}_2$

$$\boxed{\begin{aligned} p_{xi}(\tau) &= p_{xi}(0) - \tau \frac{1}{\epsilon_0}\frac{4}{ab} w \sum_j \sum_l \sum_m \frac{\alpha_l}{\gamma_{lm}^2} \sin(\alpha_l x_j)\sin(\beta_m y_j)\cos(\alpha_l x_i)\sin(\beta_m y_i) \\ p_{yi}(\tau) &= p_{yi}(0) - \tau \frac{1}{\epsilon_0}\frac{4}{ab} w \sum_j \sum_l \sum_m \frac{\beta_m}{\gamma_{lm}^2} \sin(\alpha_l x_j)\sin(\beta_m y_j)\sin(\alpha_l x_i)\cos(\beta_m y_i) \end{aligned}}$$

Symplectic Particle-In-Cell Model (1)

$$p_{xi}(\tau) = p_{xi}(0) - \tau 4\pi K \frac{4}{ab}\frac{1}{N_p}\sum_{j=1}^{N_p}\sum_{l=1}^{N_l}\sum_{m=1}^{N_m}\frac{1}{\gamma_{lm}^2}\frac{1}{\Delta x \Delta y}\int_0^a\int_0^b S(x-x_j)S(y-y_j)\sin(\alpha_l x)\sin(\beta_m y)dxdy$$
$$\times \frac{1}{\Delta x \Delta y}\int_0^a\int_0^b \frac{\partial S(x-x_i)}{\partial x_i} S(y-y_i)\sin(\alpha_l x)\sin(\beta_m y)dxdy,$$

$$p_{yi}(\tau) = p_{yi}(0) - \tau 4\pi K \frac{4}{ab}\frac{1}{N_p}\sum_{j=1}^{N_p}\sum_{l=1}^{N_l}\sum_{m=1}^{N_m}\frac{1}{\gamma_{lm}^2}\frac{1}{\Delta x \Delta y}\int_0^a\int_0^b S(x-x_j)S(y-y_j)\sin(\alpha_l x)\sin(\beta_m y)dxdy$$
$$\times \frac{1}{\Delta x \Delta y}\int_0^a\int_0^b S(x-x_i)\frac{\partial S(y-y_i)}{\partial y_i}\sin(\alpha_l x)\sin(\beta_m y)dxdy,$$

$$p_{xi}(\tau) = p_{xi}(0) - \tau 4\pi K \frac{4}{ab}\frac{1}{N_p}\sum_{j=1}^{N_p}\sum_{l=1}^{N_l}\sum_{m=1}^{N_m}\frac{1}{\gamma_{lm}^2}\sum_{I'}\sum_{J'} S(x_{I'}-x_j)S(y_{J'}-y_j)\sin(\alpha_l x_{I'})\sin(\beta_m y_{J'})$$
$$\times \sum_I\sum_J \frac{\partial S(x_I-x_i)}{\partial x_i} S(y_J-y_i)\sin(\alpha_l x_I)\sin(\beta_m y_J),$$

$$p_{yi}(\tau) = p_{yi}(0) - \tau 4\pi K \frac{4}{ab}\frac{1}{N_p}\sum_{j=1}^{N_p}\sum_{l=1}^{N_l}\sum_{m=1}^{N_m}\frac{1}{\gamma_{lm}^2}\sum_{I'}\sum_{J'} S(x_{I'}-x_j)S(y_{J'}-y_j)\sin(\alpha_l x_{I'})\sin(\beta_m y_{J'})$$
$$\times \sum_I\sum_J S(x_I-x_i)\frac{\partial S(y_I-y_i)}{\partial y_i}\sin(\alpha_l x_I)\sin(\beta_m y_J),$$

Symplectic PIC Model (2)

Define charge density on grid as:

$$\bar{\rho}(x_{I'}, y_{J'}) = \frac{1}{N_p} \sum_{j=1}^{N_p} S(x_{I'} - x_j) S(y_{J'} - y_j),$$

Space-charge $\mathcal{M}_2$

$$p_{xi}(\tau) = p_{xi}(0) - \tau 4\pi K \sum_I \sum_J \frac{\partial S(x_I - x_i)}{\partial x_i} S(y_J - y_i)$$

$$\times \left[\frac{4}{ab} \sum_{l=1}^{N_l} \sum_{m=1}^{N_m} \frac{1}{\gamma_{lm}^2} \sum_{I'} \sum_{J'} \bar{\rho}(x_{I'}, y_{J'}) \sin(\alpha_l x_{I'}) \sin(\beta_m y_{J'}) \sin(\alpha_l x_I) \sin(\beta_m y_J) \right],$$

$$p_{yi}(\tau) = p_{yi}(0) - \tau 4\pi K \sum_I \sum_J S(x_I - x_i) \frac{\partial S(y_I - y_i)}{\partial y_i}$$

$$\times \left[\frac{4}{ab} \sum_{l=1}^{N_l} \sum_{m=1}^{N_m} \frac{1}{\gamma_{lm}^2} \sum_{I'} \sum_{J'} \bar{\rho}(x_{I'}, y_{J'}) \sin(\alpha_l x_{I'}) \sin(\beta_m y_{J'}) \sin(\alpha_l x_I) \sin(\beta_m y_J) \right].$$

Symplectic PIC Model (3)

Define potential on grid as:

$$\phi(x_I, y_J) = \frac{4}{ab}\sum_{l=1}^{N_l}\sum_{m=1}^{N_m}\frac{1}{\gamma_{lm}^2}\sum_{I'}\sum_{J'}\bar{\rho}(x_{I'}, y_{J'})\sin(\alpha_l x_{I'})\sin(\beta_m y_{J'})\sin(\alpha_l x_I)\sin(\beta_m y_J).$$

$\mathcal{M}_2$ →

$$\boxed{\begin{aligned} p_{xi}(\tau) &= p_{xi}(0) - \tau 4\pi K \sum_I \sum_J \frac{\partial S(x_I - x_i)}{\partial x_i} S(y_J - y_i)\phi(x_I, y_J) \\ p_{yi}(\tau) &= p_{yi}(0) - \tau 4\pi K \sum_I \sum_J S(x_I - x_i)\frac{\partial S(y_J - y_i)}{\partial y_i}\phi(x_I, y_J) \end{aligned}}$$

$$S(x_I - x_i) = \begin{cases} \frac{3}{4} - \left(\frac{x_i - x_I}{\Delta x}\right)^2, & |x_i - x_I| \leq \Delta x/2, \\ \frac{1}{2}\left(\frac{3}{2} - \frac{|x_i - x_I|}{\Delta x}\right)^2, & \Delta x/2 < |x_i - x_I| \leq 3/2\Delta x, \\ 0 & \text{otherwise,} \end{cases}$$

$$\frac{\partial S(x_I - x_i)}{\partial x_i} = \begin{cases} -2\left(\frac{x_i - x_I}{\Delta x}\right)/\Delta x, & |x_i - x_I| \leq \Delta x/2, \\ \left(-\frac{3}{2} + \frac{(x_i - x_I)}{\Delta x}\right)/\Delta x, & \Delta x/2 < |x_i - x_I| \leq 3/2\Delta x, x_i > x_I, \\ \left(\frac{3}{2} + \frac{(x_i - x_I)}{\Delta x}\right)/\Delta x, & \Delta x/2 < |x_i - x_I| \leq 3/2\Delta x, x_i \leq x_I, \\ 0 & \text{otherwise.} \end{cases}$$

Non-Symplectic PIC Model

$$\frac{d\mathbf{r}_i}{ds} = \mathbf{p}_i$$
$$\frac{d\mathbf{p}_i}{ds} = q(\mathbf{E}_i/v_0 - a_z \times \mathbf{B}_i)$$

$$\mathbf{r}(\tau/2)_i = \mathbf{r}(0)_i + \frac{1}{2}\tau\mathbf{p}_i(0)$$

$$E_x(x_I, y_J) = -\sum_{l=1}^{N_l}\sum_{m=1}^{N_m} \alpha_l \phi^{lm} \cos(\alpha_l x)\sin(\beta_m y)$$

$$E_y(x_I, y_J) = -\sum_{l=1}^{N_l}\sum_{m=1}^{N_m} \beta_m \phi^{lm} \sin(\alpha_l x)\cos(\beta_m y)$$

$$p_{xi}(\tau) = p_{xi}(0) + \tau(\frac{qE_x^{ext}}{v_0} - qB_y^{ext}) + \tau 4\pi K \sum_I \sum_J S(x_I - x_i)S(y_J - y_i)E_x(x_I, y_J)$$

$$p_{yi}(\tau) = p_{yi}(0) + \tau(\frac{qE_y^{ext}}{v_0} + qB_x^{ext}) + \tau 4\pi K \sum_I \sum_J S(x_I - x_i)S(y_J - y_i)E_y(x_I, y_J)$$

$$\mathbf{r}(\tau)_i = \mathbf{r}(\tau/2)_i + \frac{1}{2}\tau\mathbf{p}_i(\tau)$$

Benchmark Case 1: FODO Lattice, Below 2nd Order Envelop Instability

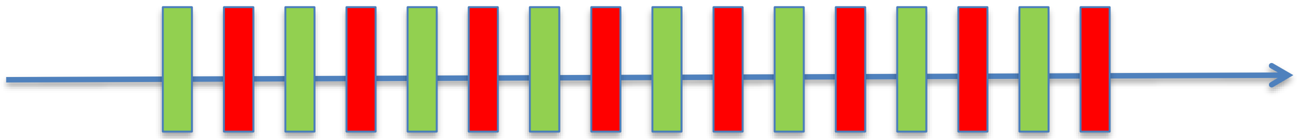

- 1 GeV proton beam
- FODO lattice
- 0 current phase advance: 85 degrees
- Initial 4D Gaussian distribution

Significant Difference in Final 4D Emittances Between the Symplectic and the Non-Symplectic Methods (Strong Space-Charge: Phase Advance Change 85 -> 42)

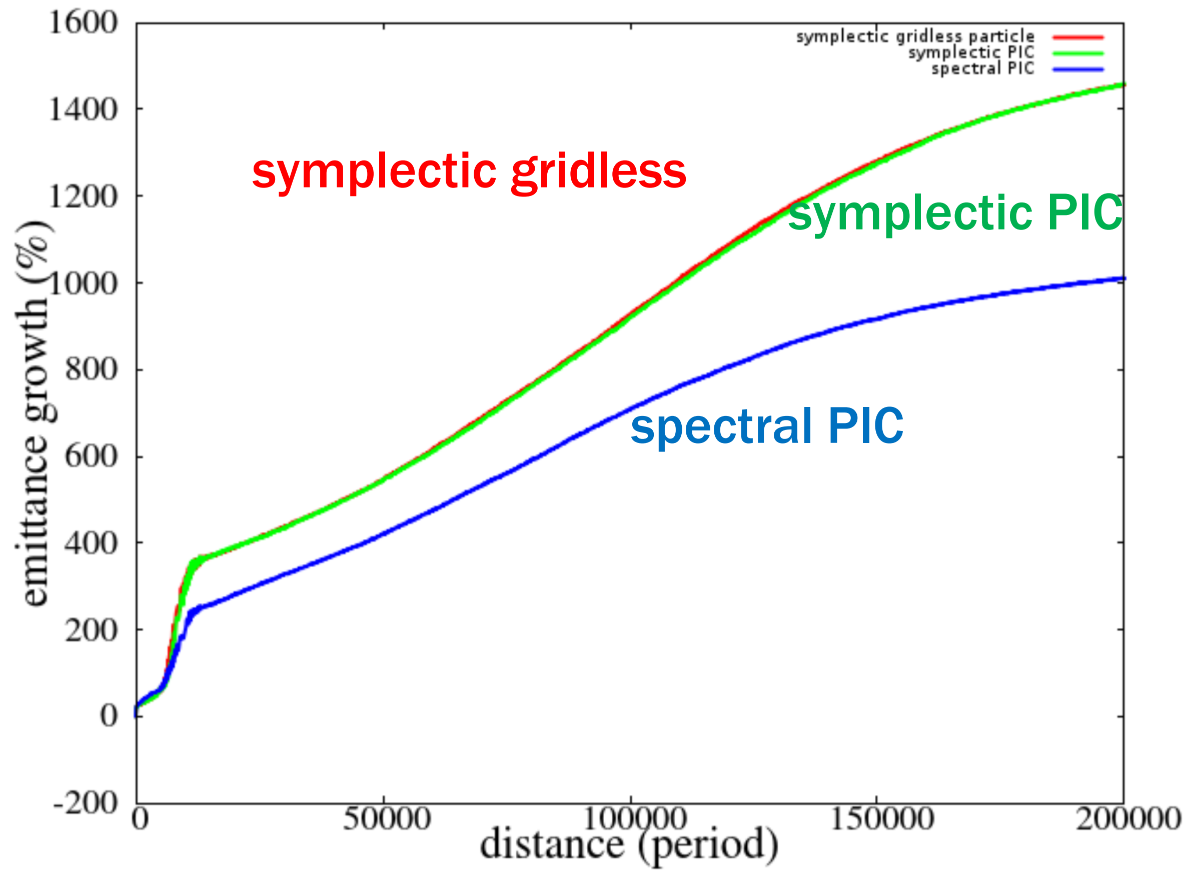

Two symplectic approaches show good agreement.

Final Beam X-Px Phase Spaces Have Similar Shapes
Non-Symplectic Model Has Smaller Area

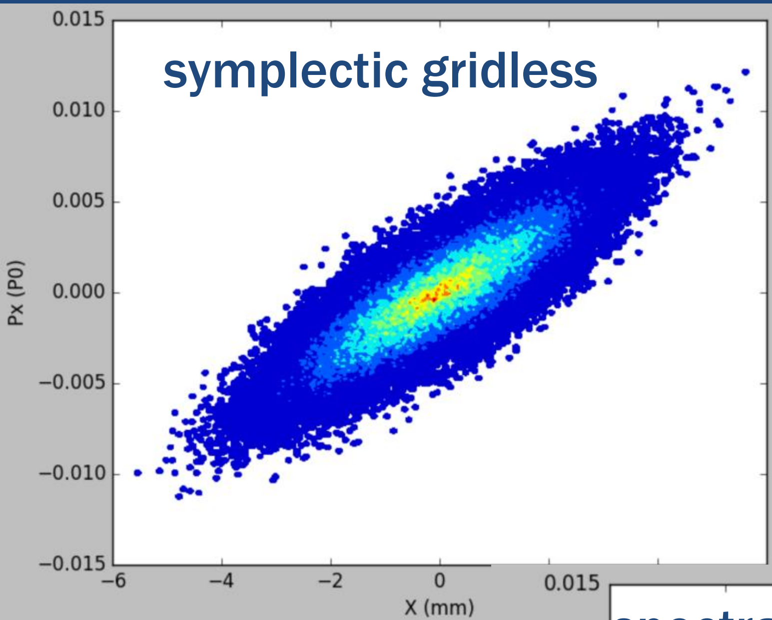

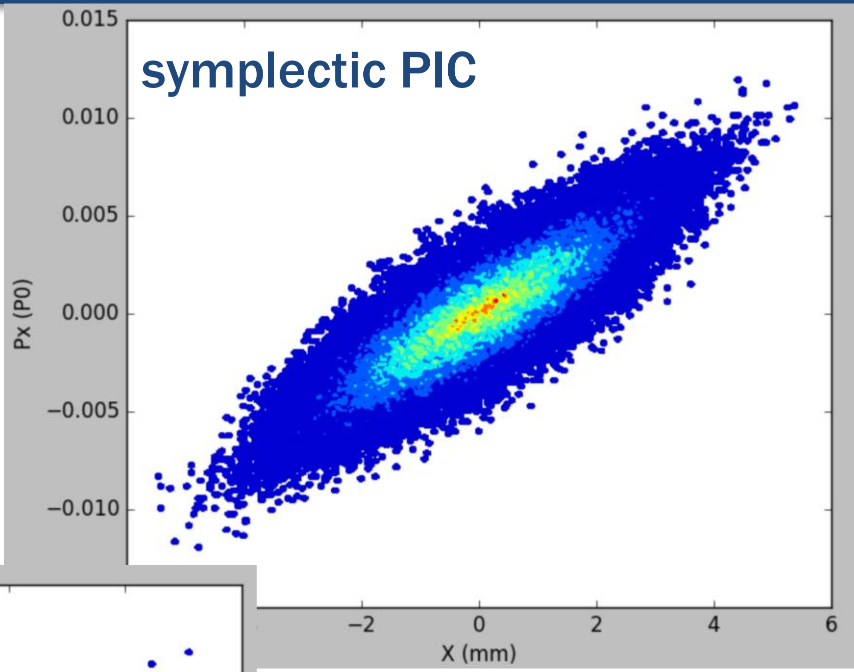

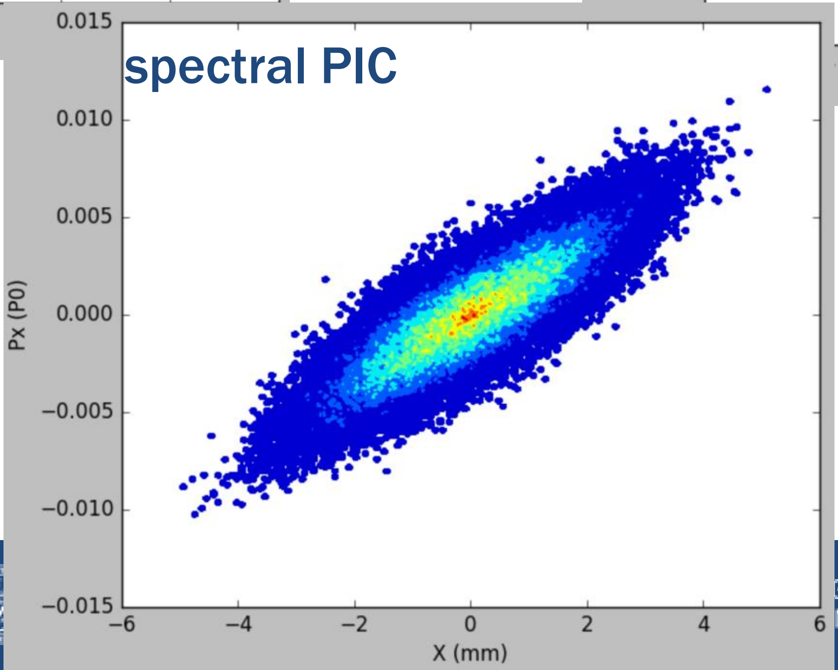

Final Y-Py Phase Space Show Similar Shapes

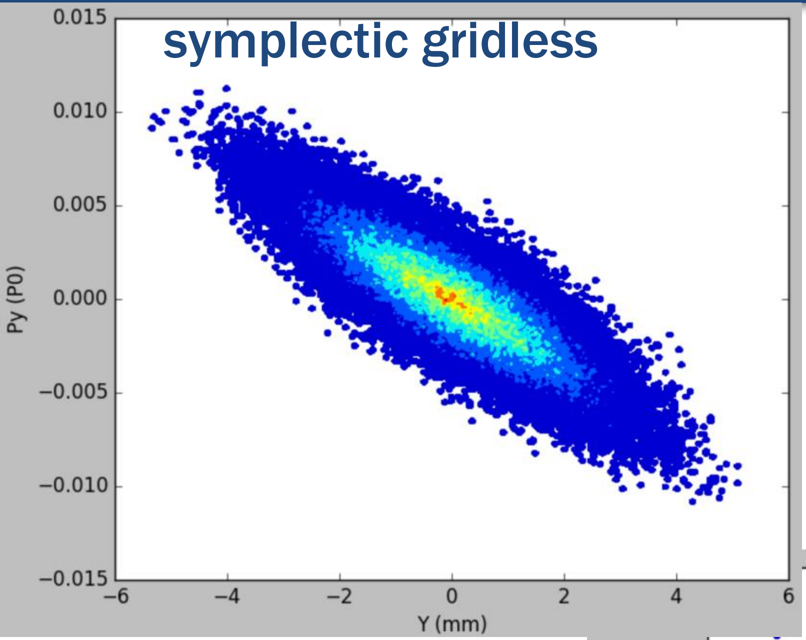

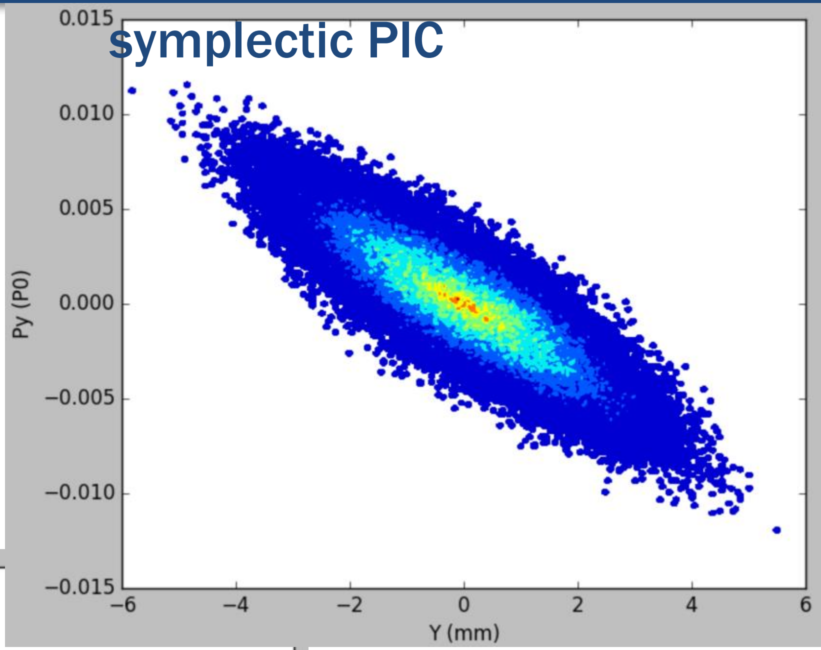

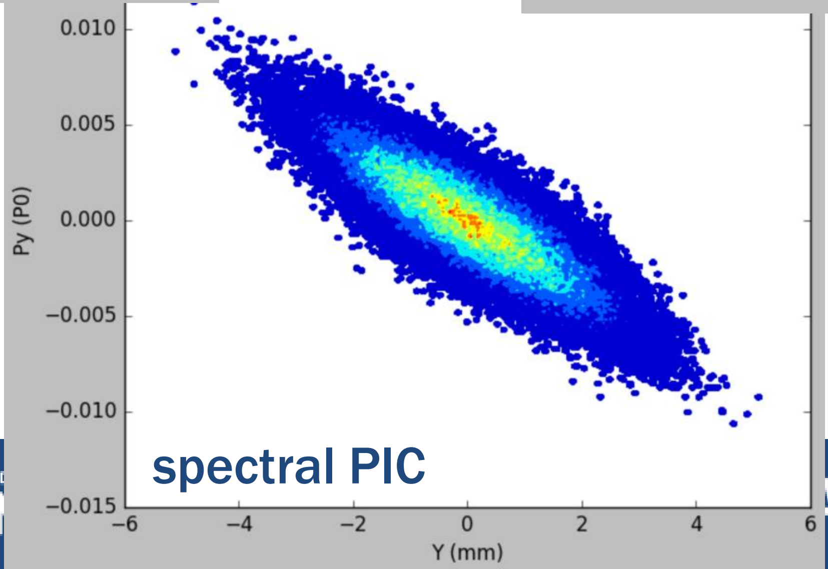

Horizontal and Vertical Density Profiles from the Symplectic Gridless Model, the Symplectic PIC Model, and the Non-Symplectic Spectral PIC

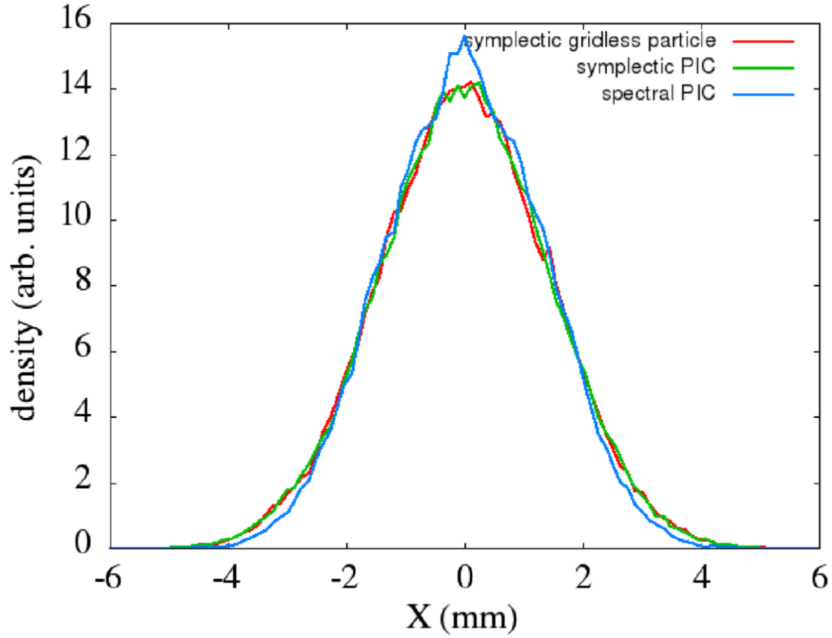

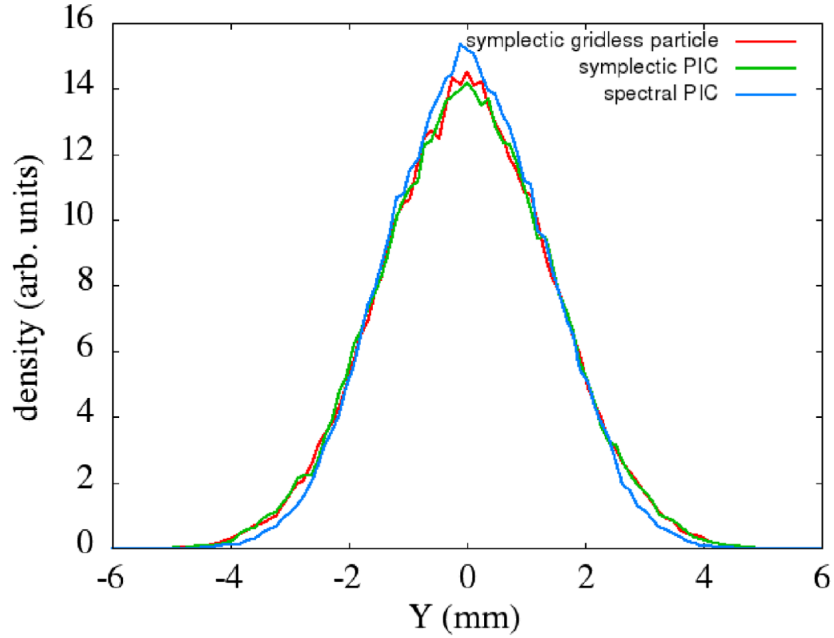

- Two symplectic solvers produce similar density profiles
- Non-symplectic solver produces larger core density

Finer Step Size Needed for Non-Symplectic PIC (Symplectic PIC vs. Non-Symplectic PIC)

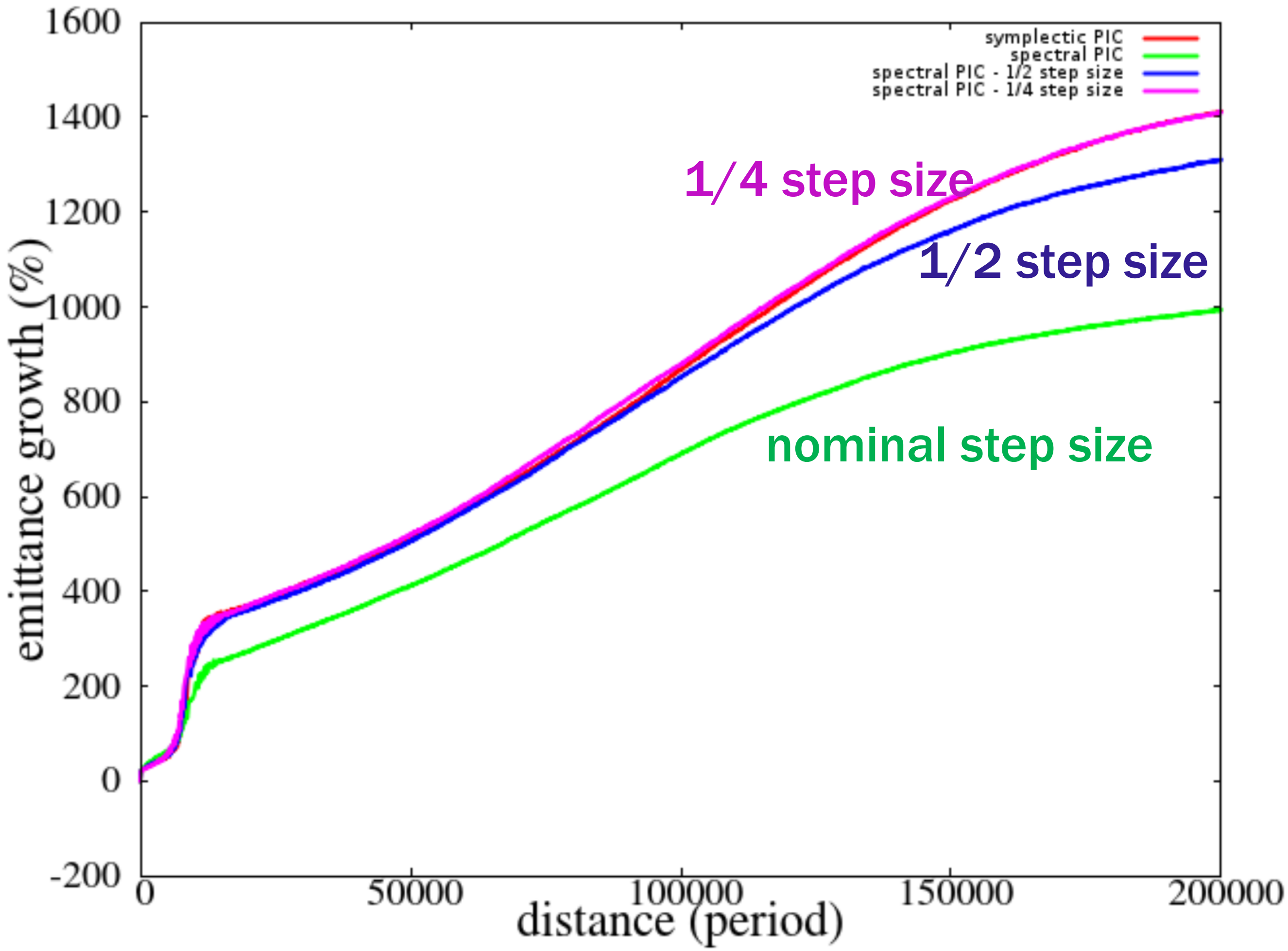

Benchmark Case 2: 1 Turn = 10 FODOs + 1 Sextupole

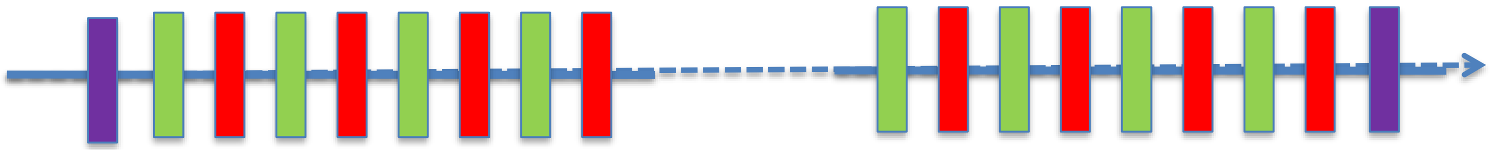

- 0 current tune 2.417, 30 A current, tune shift 0.113
- sextupole KL = 10 T/m/m

Non-Symplectic PIC Shows Much Less Emittance Growth Compared with Two Symplectic Models (4D Emittance Evolution with Different Currents)

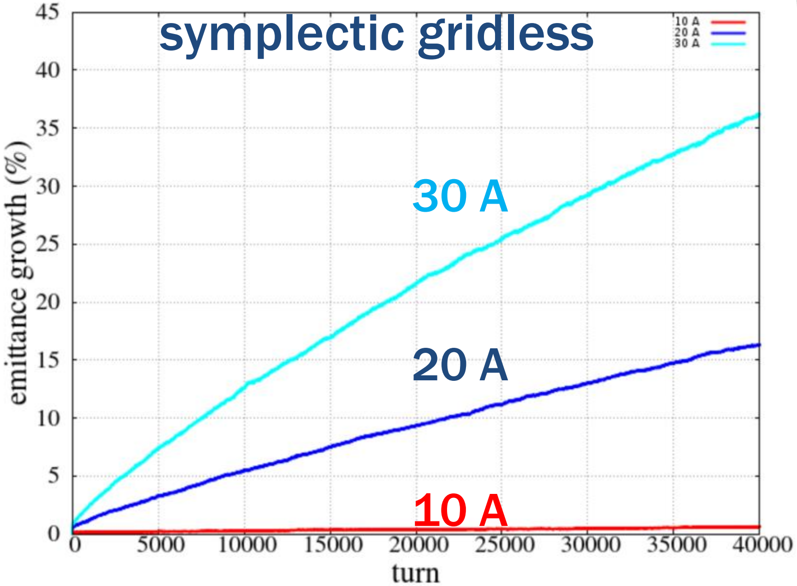

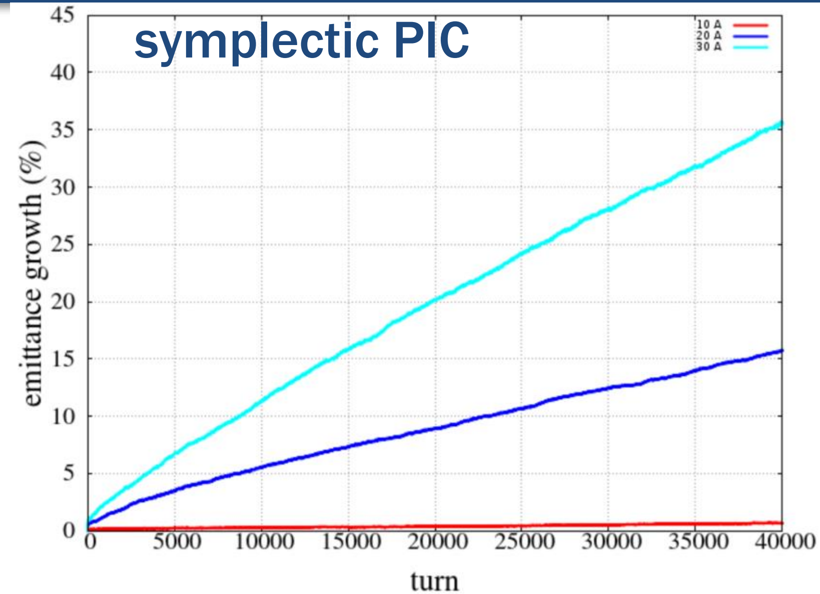

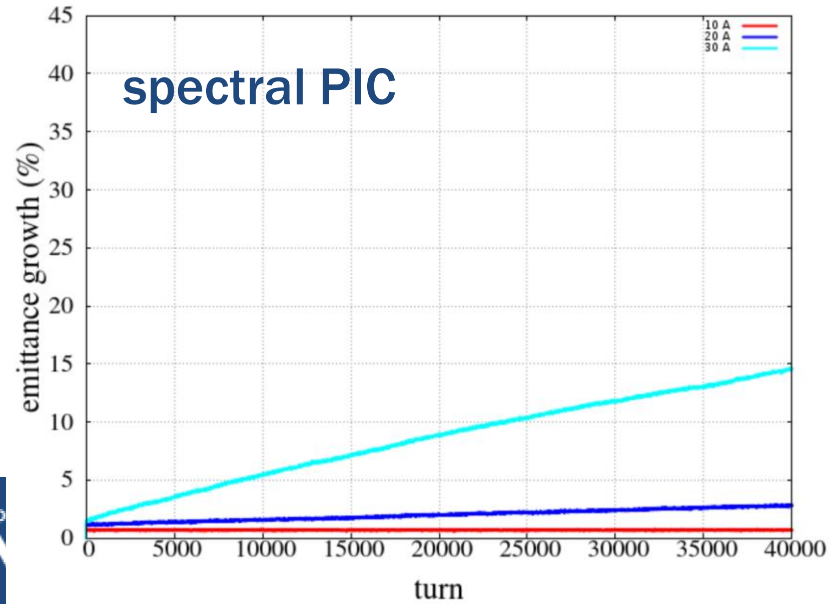

Final Beam X-Px Phase Spaces Have Similar Shapes

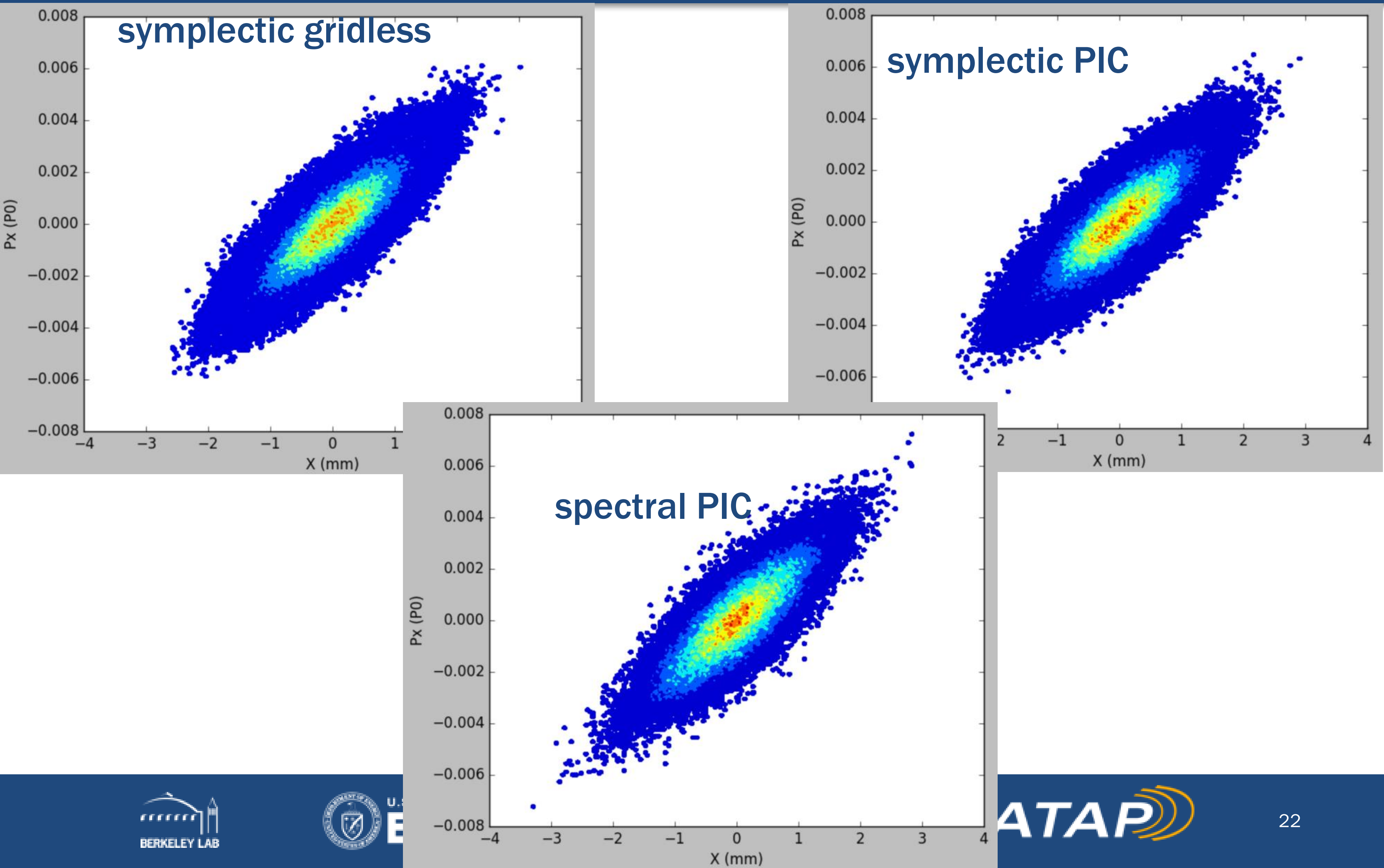

Final Beam Y-Py Phase Spaces Have Similar Shapes

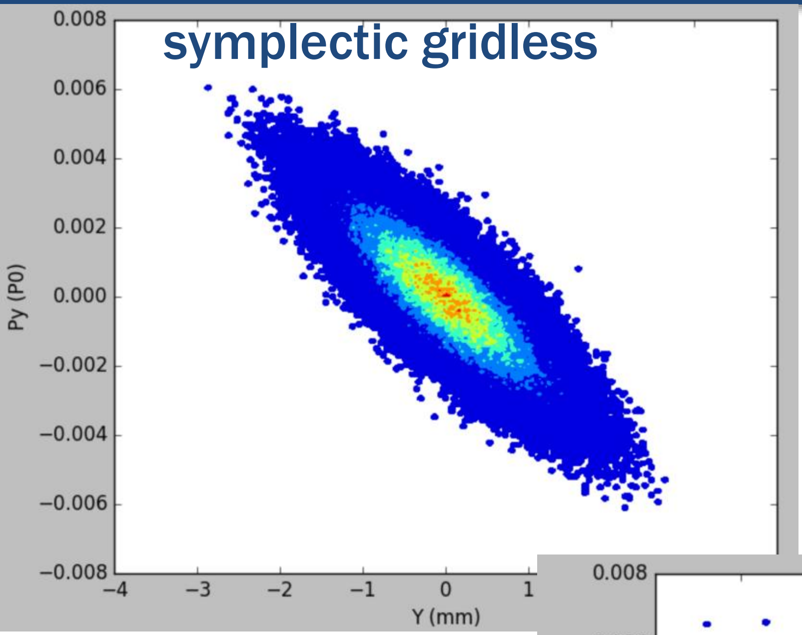

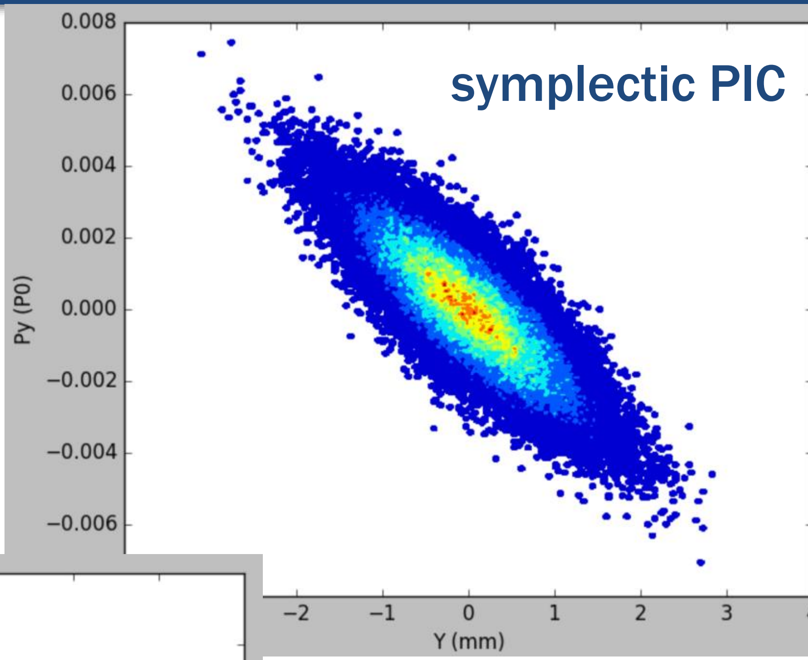

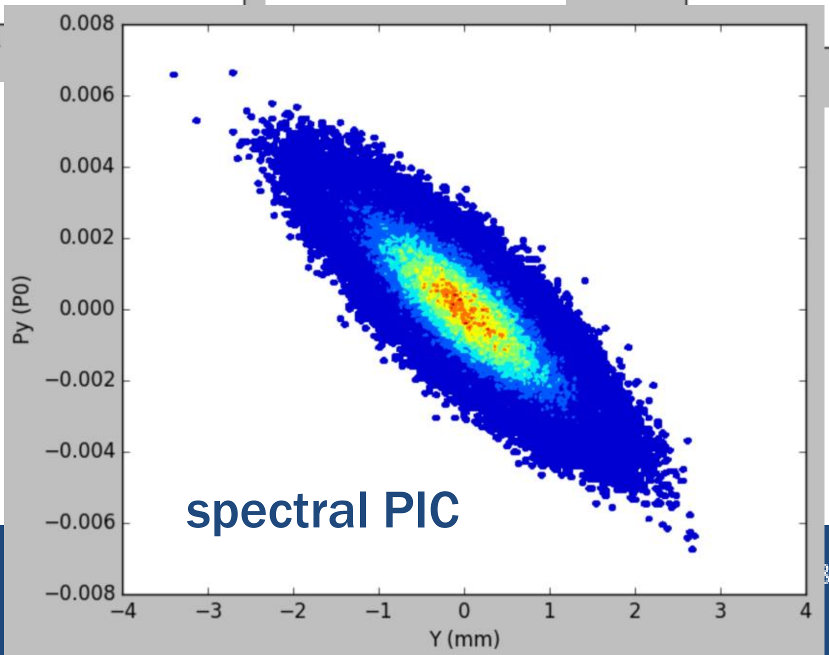

Comparison of Density Profiles

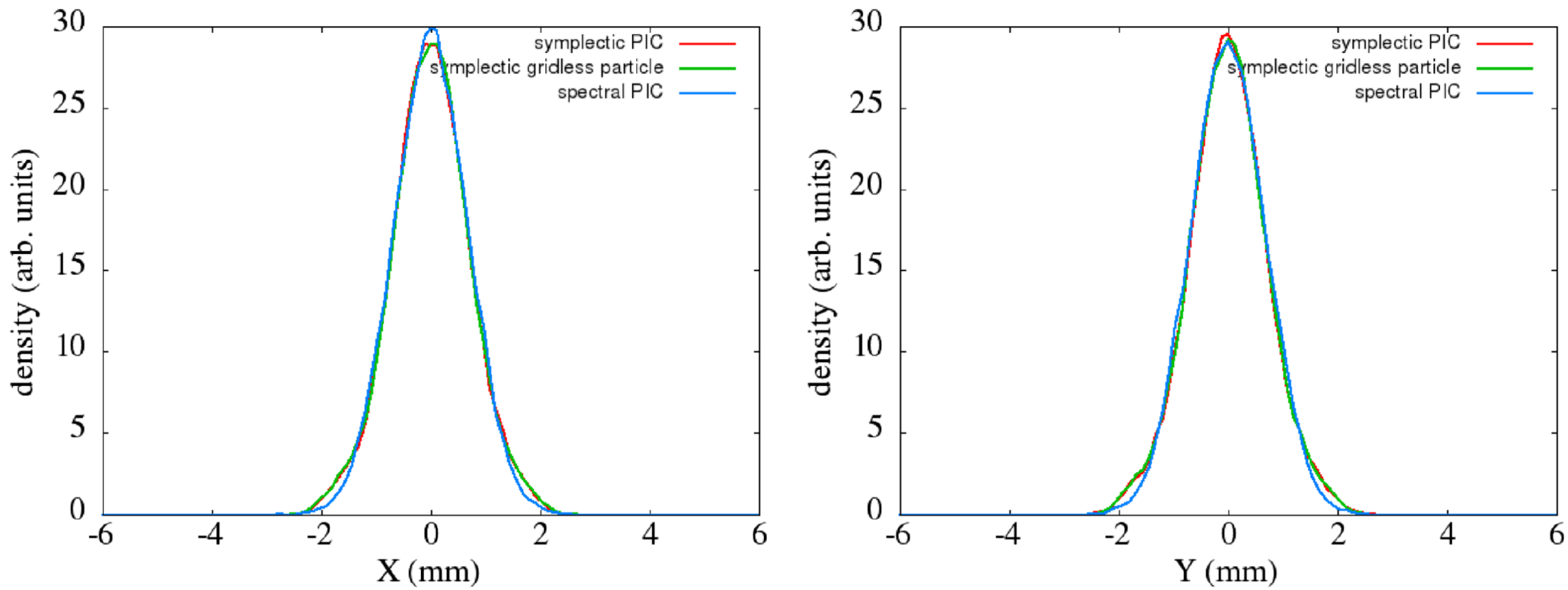

- Two symplectic solvers produce similar density profiles
- Non-symplectic solver produces larger less shoulder

Extra Numerical Emittance Growth with Small Number of Macroparticles

sextupole KL = 0, 64x64 modes

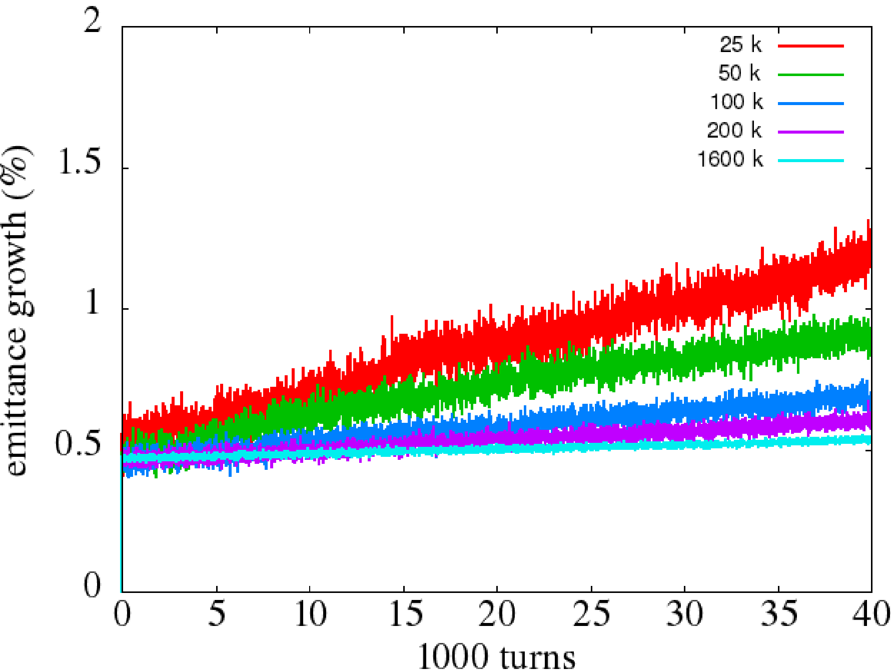

sextupole KL = 10, 64x64 modes

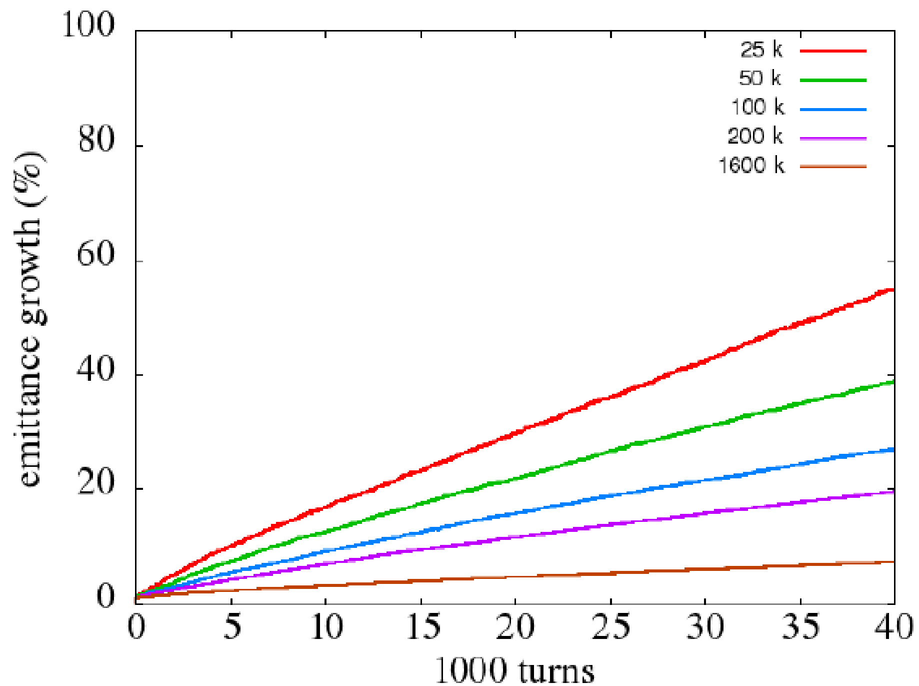

- Little emittance growth in the linear lattice
- Small emittance growth driven by the 3rd order resonance
- Sufficient number of macroparticles needed to suppress numerical emittance growth

Understand the Numerical Emittance Growth from a 1D Model

The *smooth* and the reconstructed Gaussian distributions from macroparticle sampling with *linear*, *quadratic*, and *Gaussian kernel* deposition

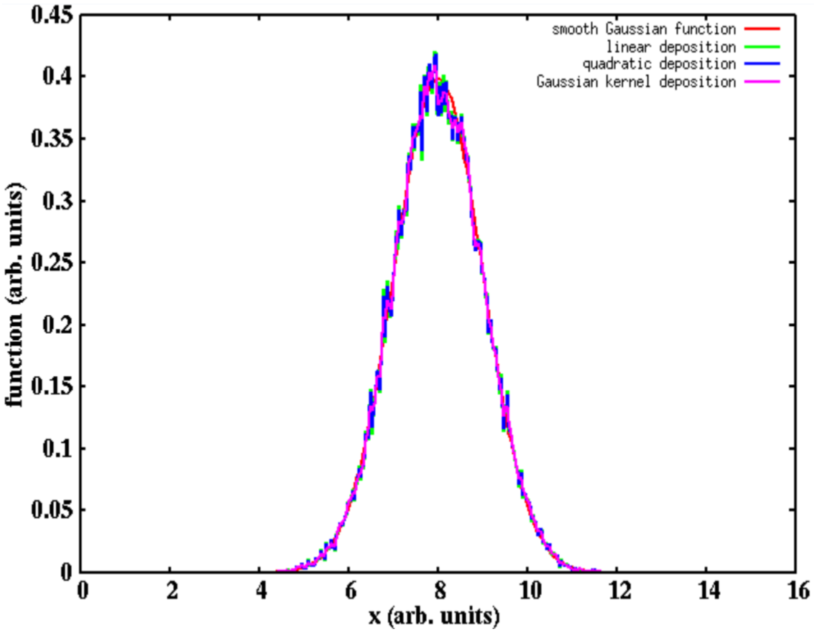

The mode amplitude of the smooth and the reconstructed Gaussian distributions from macroparticle sampling with linear, quadratic, and Gaussian kernel deposition

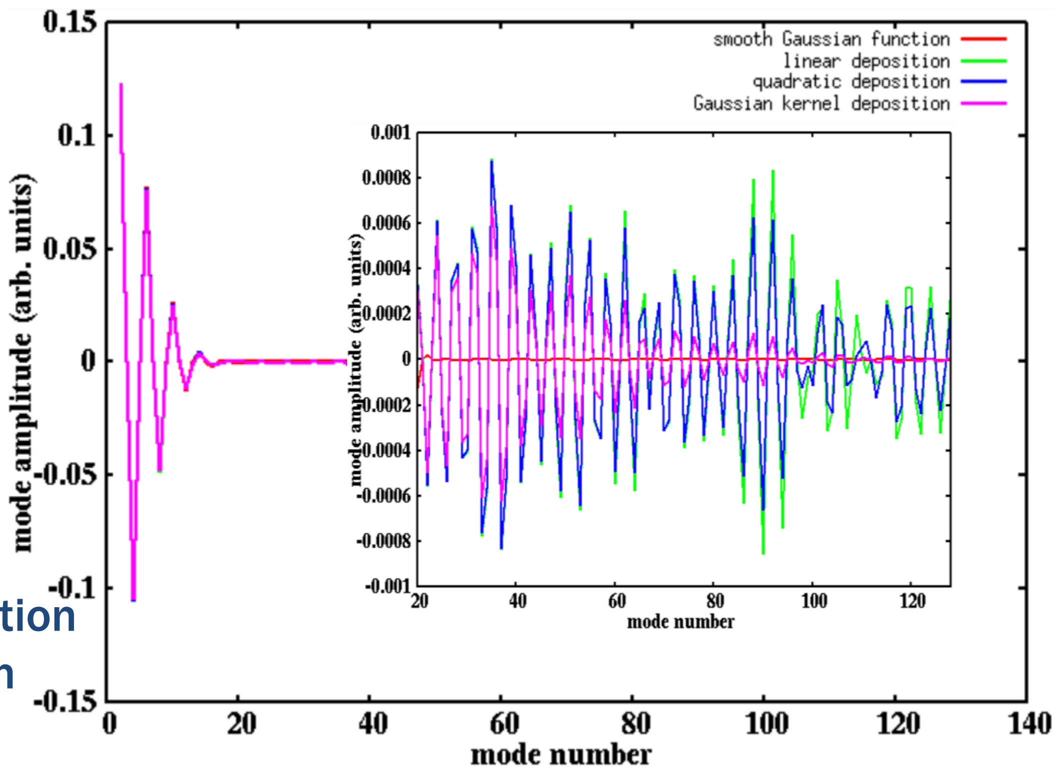

- Much larger mode amplitude fluctuation from the macroparticle depositions than that from the smooth distribution

Quantify the Mode Amplitude Fluctuation with Standard Deviation

$$\rho^l = \frac{1}{N_p}\frac{2}{N_g\Delta x}\sum_i\sum_I S(x_I - x_i)\sin(\alpha_l x_i)$$

$$var(\rho^l) = \frac{1}{N_p}var(\frac{2}{N_g\Delta x}\sum_I S(x_I - x_i)\sin(\alpha_l x_i))$$

$$var(\frac{2}{N_g\Delta x}\sum_I S(x_I - x_i)\sin(\alpha_l x_i)) \approx \frac{1}{N_p}(\frac{2}{N_g\Delta x})^2\sum_i[\sum_I S(x_I - x_i)\sin(\alpha_l x_i)]^2 - (\rho^l)^2$$

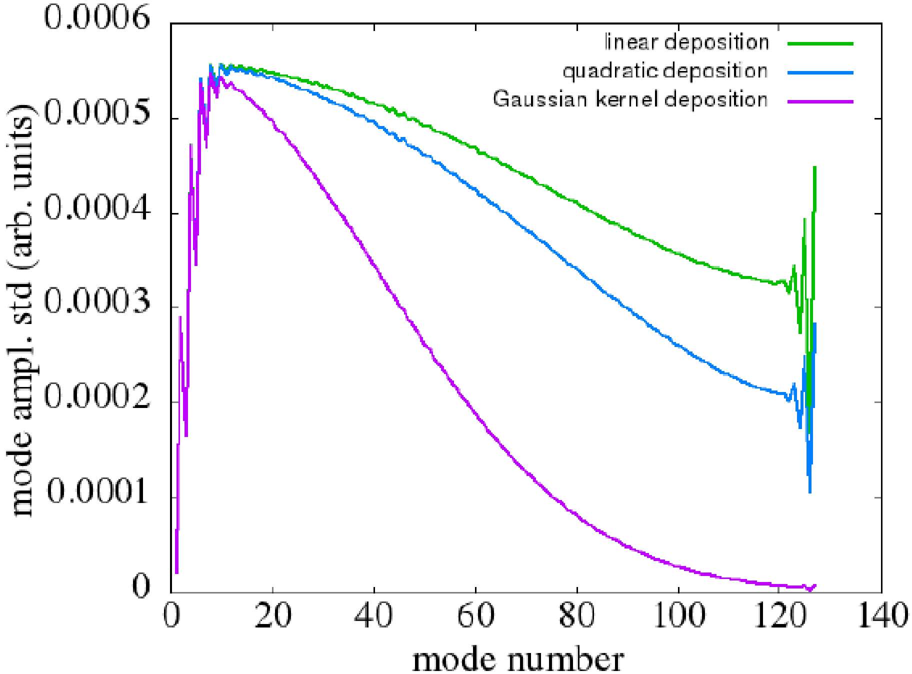

➢ **Higher order macroparticle deposition scheme leads to smaller fluctuation**

Mode Amplitude Fluctuation Decreases with the Increase of Macroparticle Number

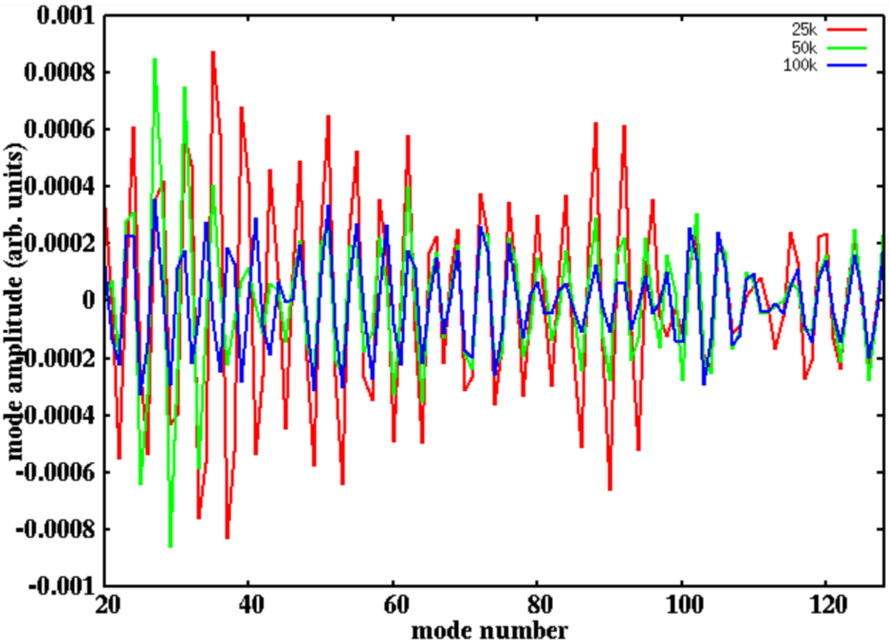

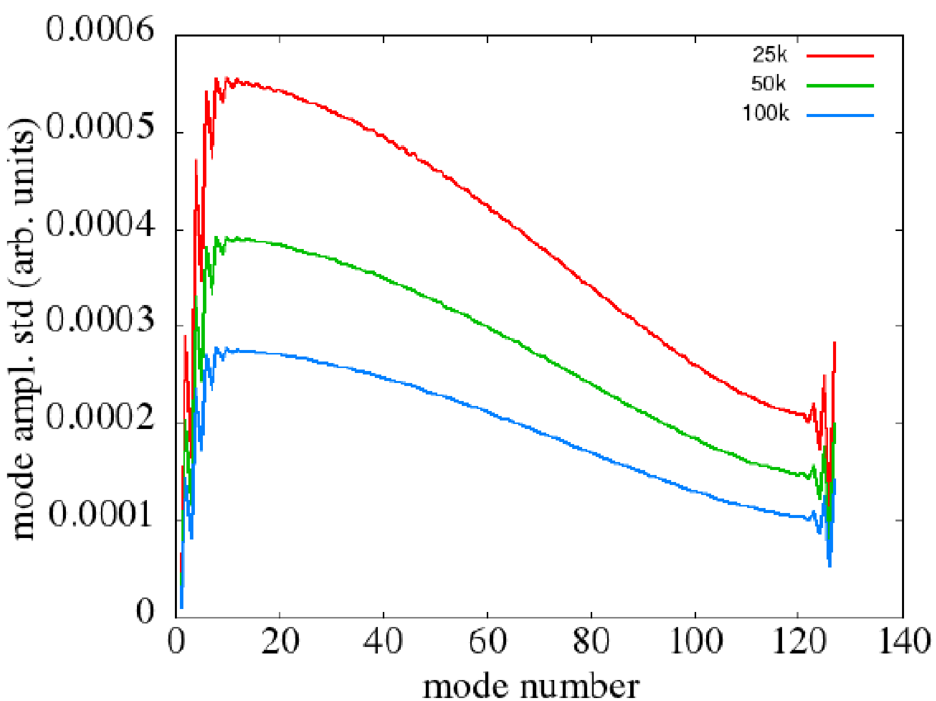

- Fluctuation standard deviation ~ 1/sqrt(Np)

Mode Amplitude Fluctuation Increases with the Increase of Grid Number

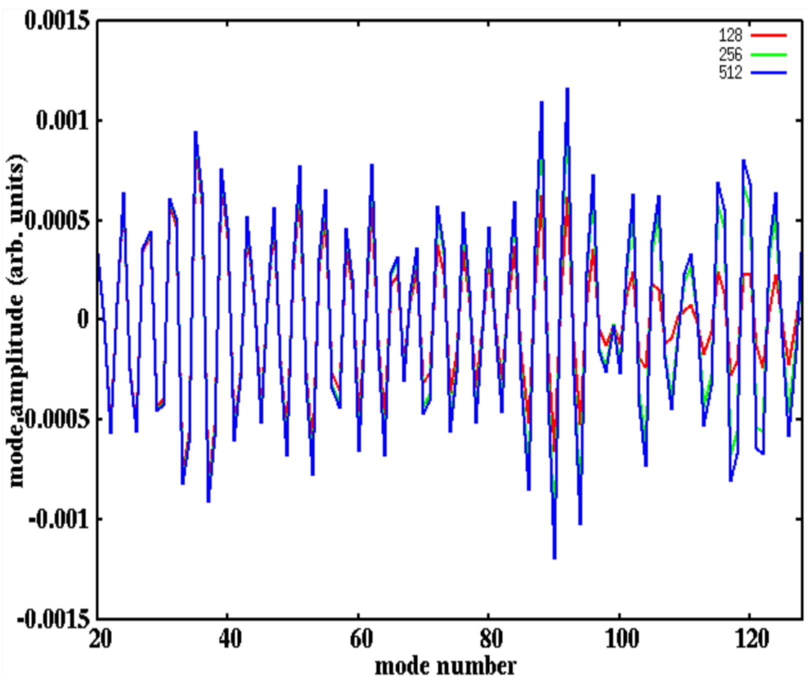

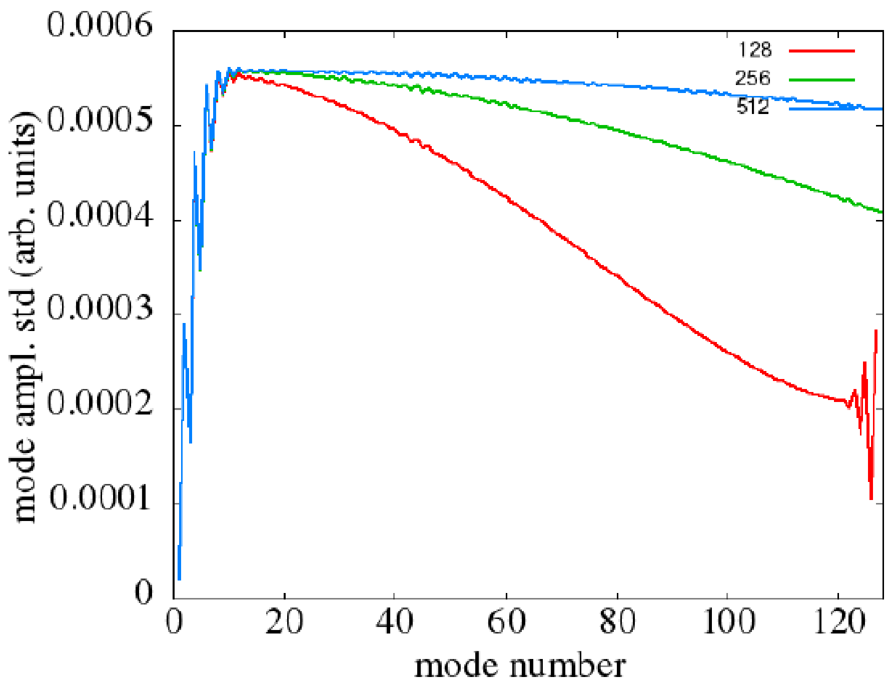

- Grid number mainly affects mode number > 10
- Larger grid number results in larger fluctuation

Numerical Errors of in the Charge Density Distribution from Macroparticles Results in Numerical Emittance Growth

$$\Delta\epsilon \approx (<x^2><x'\delta F> - <xx'><x\delta F>)\tau/\epsilon + \frac{1}{2}(<x^2><(\delta F)^2> - <x\delta F>^2)\tau^2/\epsilon$$

$$\frac{\Delta\epsilon}{\tau} \approx \frac{1}{2}<x^2><(\delta F)^2>\tau/\epsilon$$

sextupole KL = 0, 64x64 modes

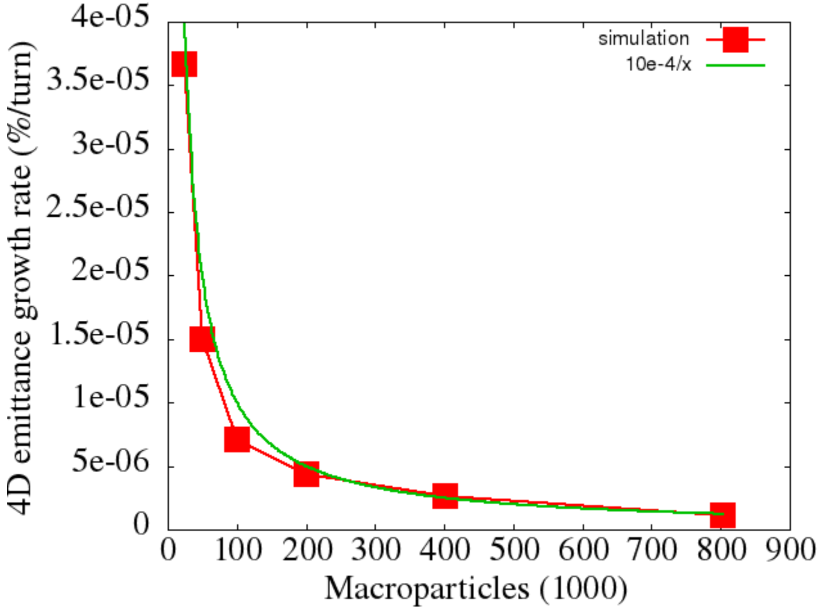

- ➢ Numerical emittance growth scales close to 1/Np as expected

sextupole KL = 10, 64x64 modes

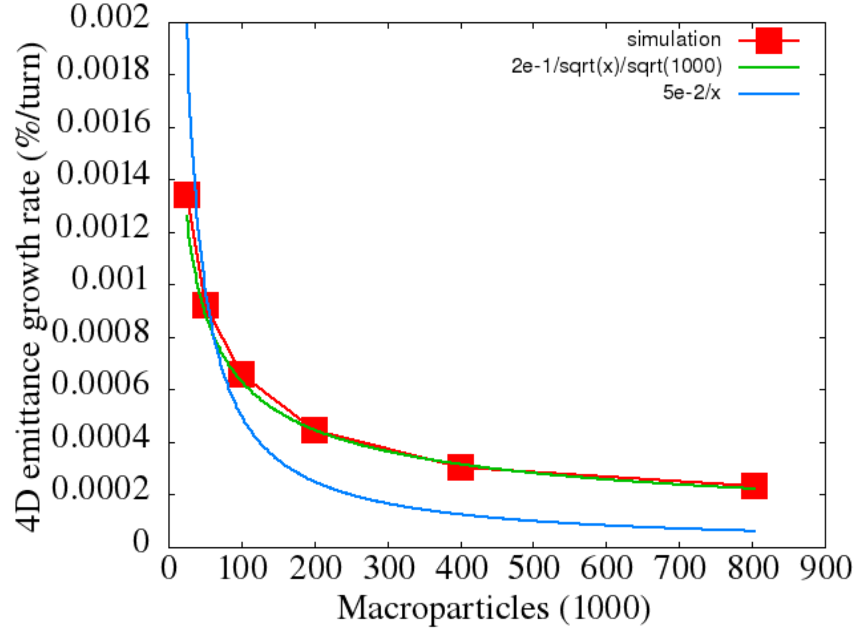

- ➢ Numerical emittance growth scales close to 1/sqrt(Np)
- ➢ The growth mechanism is more complicated

Removing Small Amplitude Fluctuation Modes Using Relative Amplitude Threshold (1)

Spectral amplitude of a 2D Gaussian density (64x64 mode)

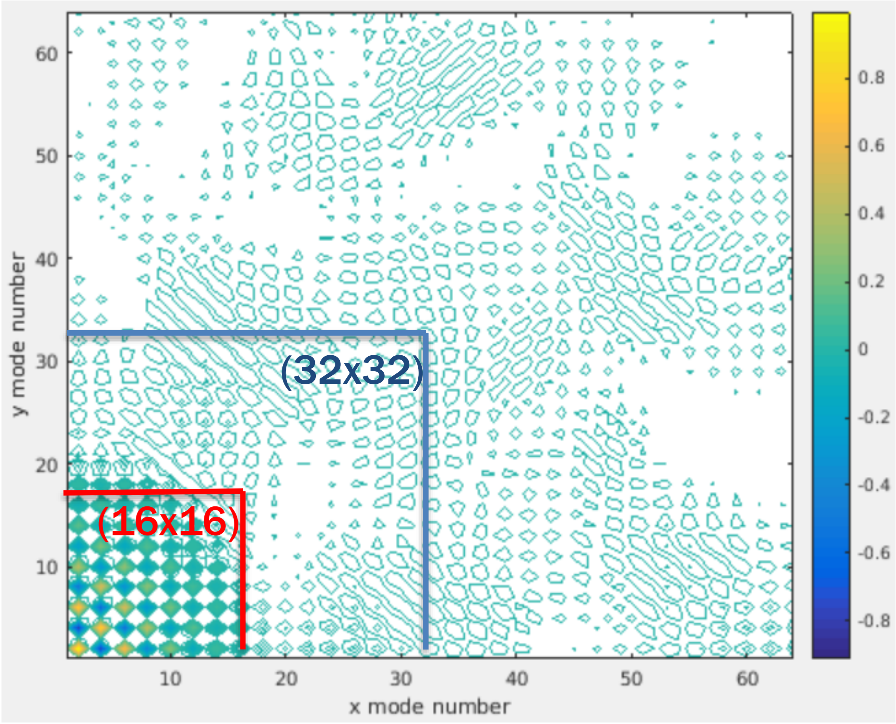

Spectral amplitude of a 2D Gaussian density with 1% threshold

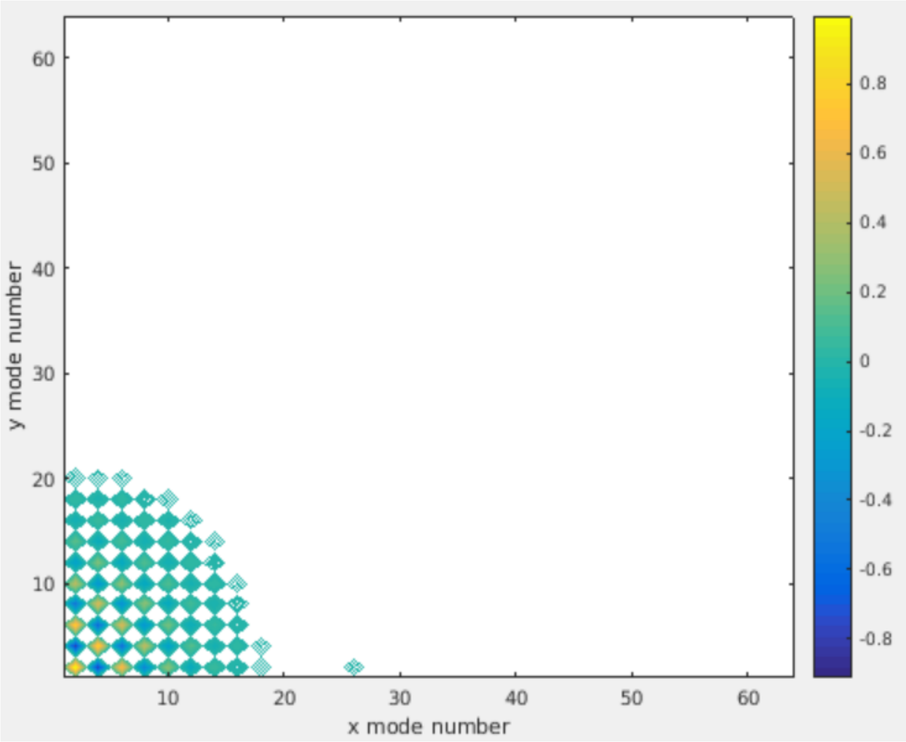

Removing Small Amplitude Fluctuation Modes Using Relative Amplitude Threshold (2)

Spectral amplitude of a 2D Gaussian density with 2 sigma threshold

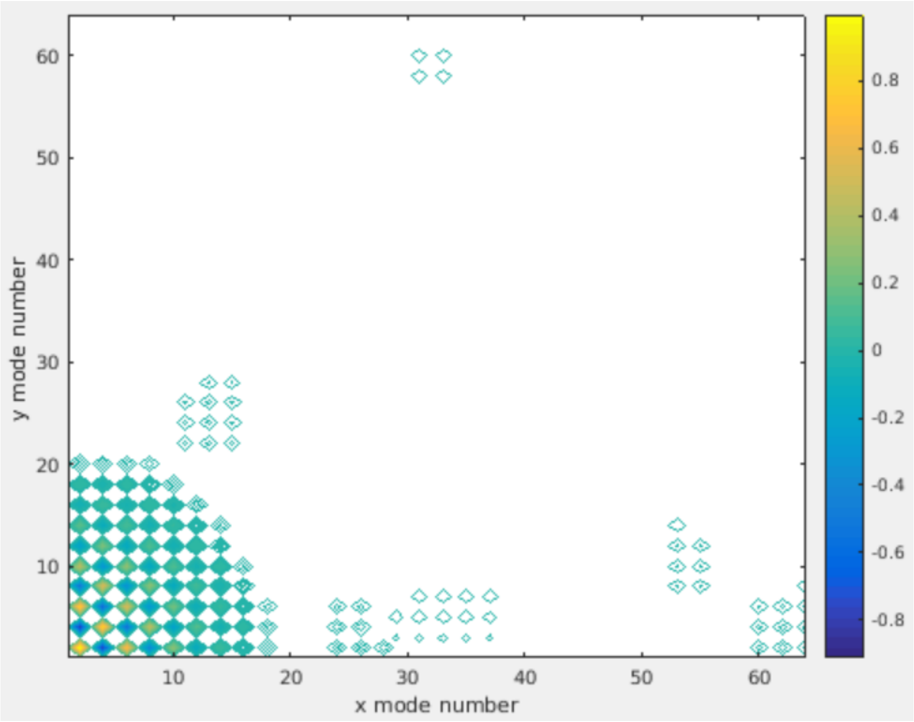

Spectral amplitude of a 2D Gaussian density with 4 sigma threshold

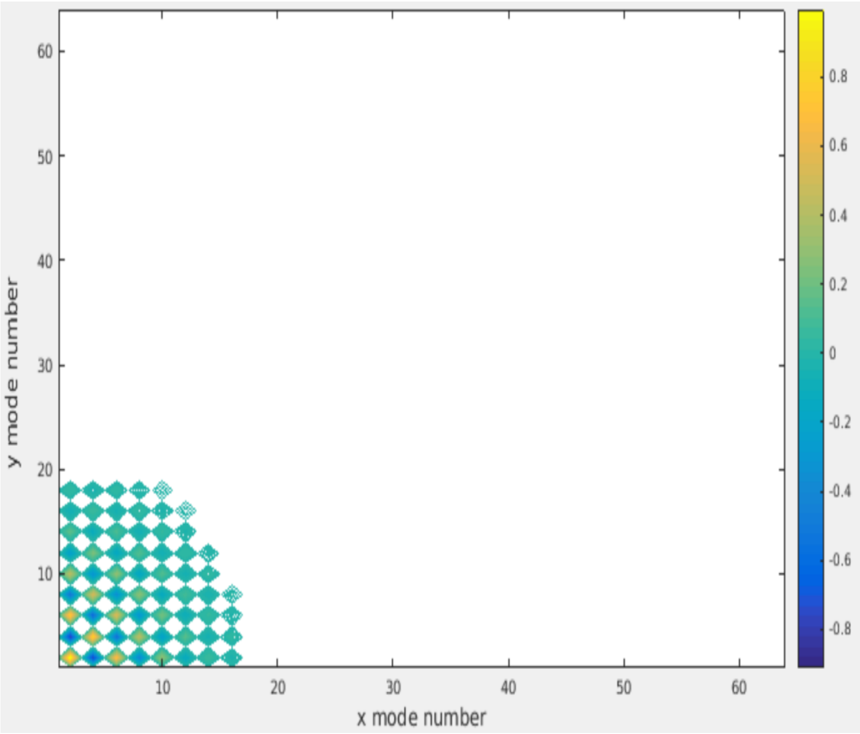

Mitigate the Numerical Emittance Growth by Removing High Frequency Modes in Linear Lattice

sextupole KL = 0, current = 30 A, 25 k macroparticles

brute force cut-off

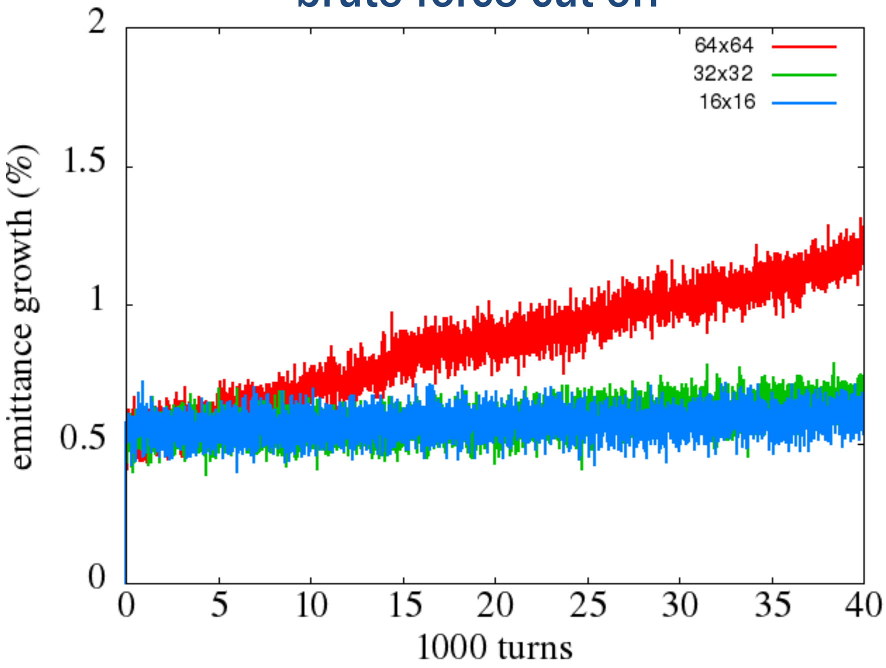

threshold filtering

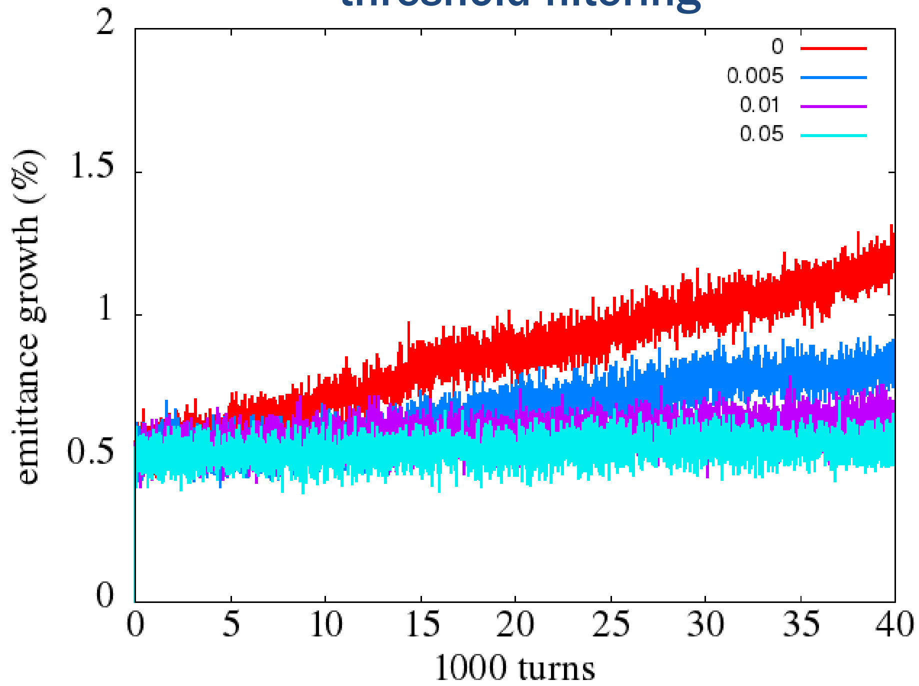

- Both numerical filters work well
- Numerical emittance growth is mainly due high frequency errors

Mitigate the Numerical Emittance Growth through Threshold Filtering in Nonlinear Lattice

sextupole KL = 10, current = 30 A, 25 k macroparticles

brute force cut-off

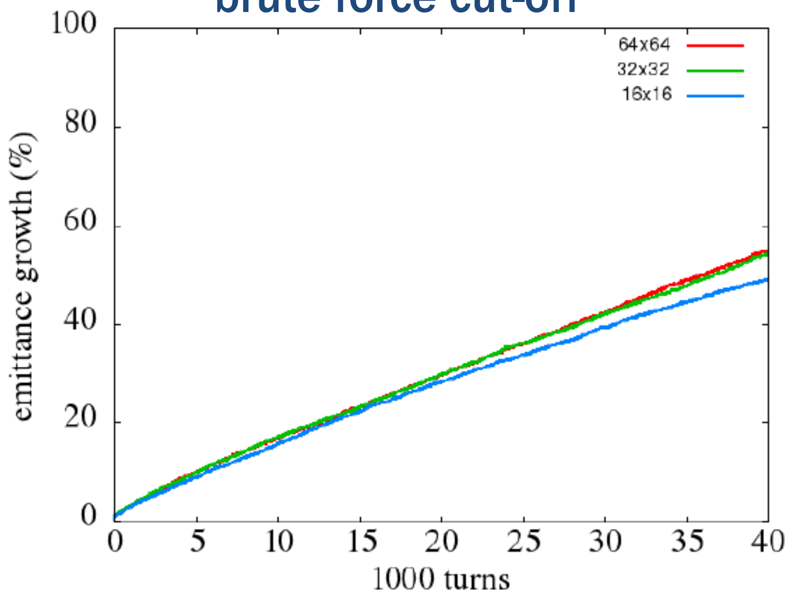

threshold filtering

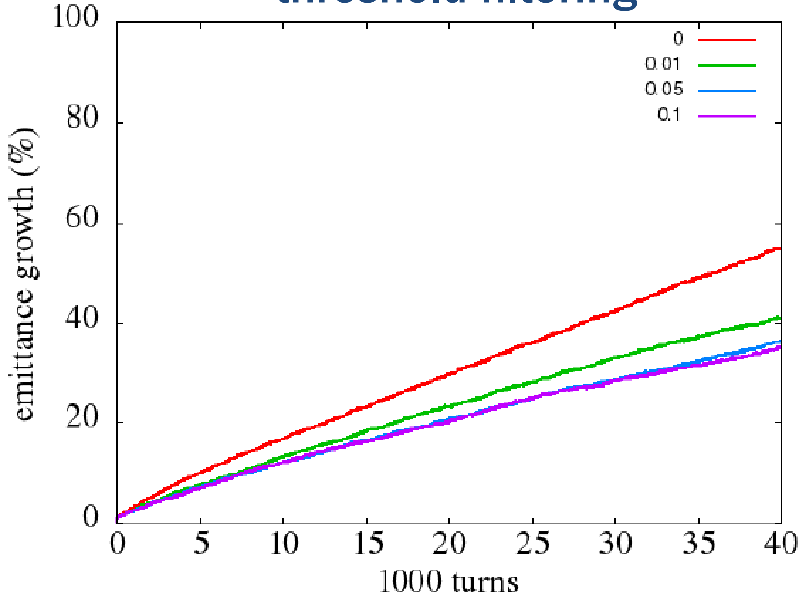

- ➢ Direct brute force cut-off filtering is not efficient
- ➢ Numerical emittance growth can be mitigated with threshold filtering
- ➢ The numerical growth is mainly due low frequency errors

Predefined Maximum Fraction and Four Sigma Threshold Filtering Yields Similar Emittance Growth

sextupole KL = 10, current = 30 A, 25 k macroparticles

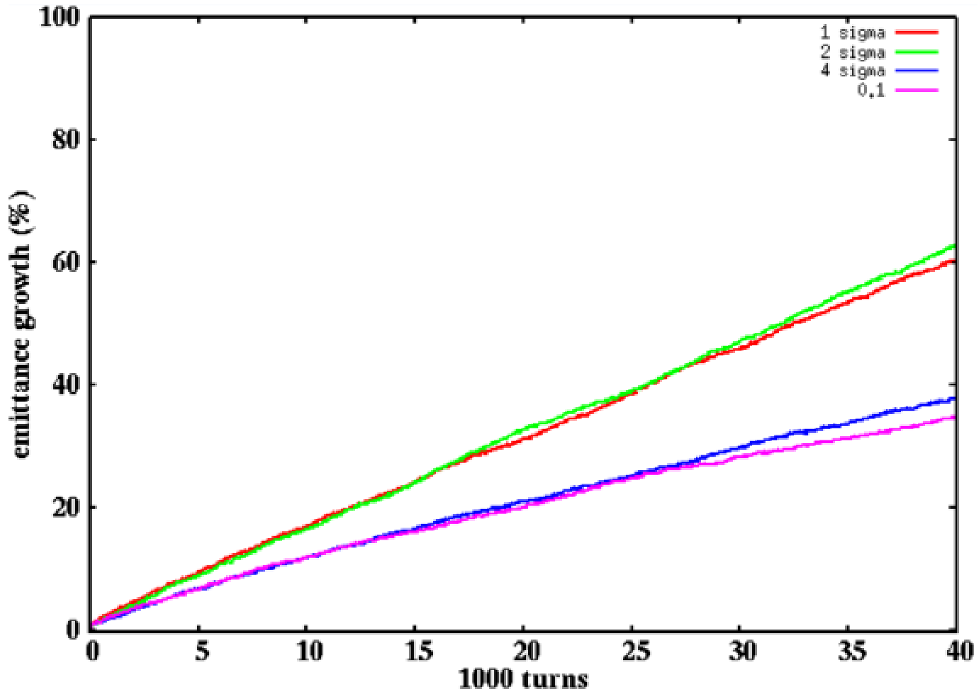

Maximum Fraction

Pro – easy to calculate the threshold value

Con – another hyperparameter

Standard Deviation

Pro – calculate the threshold value dynamically

Con – computationally expensive

Computational Complexity

- Symplectic PIC/Spetral PIC: O(Np) + O(Ng log(Ng)), parallelization can be a challenge
- Symplectic gridless particle: O(Nm Np),
  easy parallelization

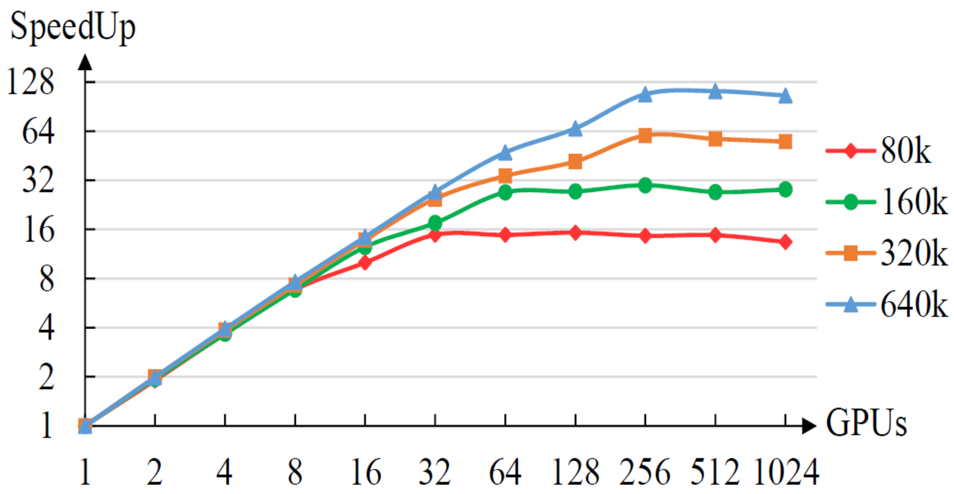

Z. Liu and J. Qiang, “Symplectic multi-particle tracking on GPUs,” Computer Physics Communications, 226, 10 (2018).

Summary

- Symplectic space-charge model will help improve the accuracy of simulation for long-term simulation.
- Numerical emittance growth from finite macroparticle sampling can be mitigated using threshold filtering in frequency domain.
- For small number of modes and particles used, the symplectic gridless particle model can be computationally efficient; otherwise, the symplectic PIC model would be more efficient.